Plasma Sources Science and Technology

PAPER

Evolutions of streamer dynamics and discharge instabilities under repetitive pulses in humid air

To cite this article: Zheng Zhao *et al* 2023 *Plasma Sources Sci. Technol.* **32** 125011

View the article online for updates and enhancements.

You may also like

- Characteristics of spatiotemporal variations of primary and secondary streamers under pulsed-voltage in air at atmospheric pressure
  Atsushi Komuro, Kento Suzuki, Keigo Yoshida et al.
- Temporal evolution and mechanism of secondary streamers in N_2/O_2 mixtures at atmospheric pressure under DC voltage
  Xinlei Zheng, Zihan Sun, Chenjie Li et al.
- Kinetic plasma chemistry model of pulsed transient spark discharge in air coupled with nanosecond time-resolved imaging and spectroscopy
  Mário Janda, Karol Hensel and Zdenko Machala

This content was downloaded from IP address 202.200.233.56 on 30/04/2024 at 10:32

Plasma Sources Sci. Technol. 32 (2023) 125011 (19pp)

https://doi.org/10.1088/1361-6595/ad0d08

Evolutions of streamer dynamics and discharge instabilities under repetitive pulses in humid air

Zheng Zhao, Qiuyu Gao, Xinlei Zheng, Haowei Zhang, Haotian Zheng, Anbang Sun* and Jiangtao Li*

School of Electrical Engineering, Xi'an Jiaotong University, Xi'an 710049, People's Republic of China

E-mail: anbang.sun@xjtu.edu.cn and li_jiangtao@xjtu.edu.cn

Received 10 May 2023, revised 30 October 2023
Accepted for publication 16 November 2023
Published 22 December 2023

Abstract

The presence of water molecules in air introduces complexities to residual charge transports and energy relaxations that may provoke streamer discharge instabilities under repetitive pulses. Evolutions of pulse-periodic positive streamer dynamics were investigated in humid air. Pulse-sequence and temporally resolved diagnostics were implemented to capture discharge evolutions. The streamer development and evolutions of charged species in humid air are qualitatively analyzed based on a 2D–0D combined simulation. Evolution features of streamer behaviors in humid air include the faster filamentation of the primary streamer, pronounced propagation selectivity to previous secondary streamers, more branches of both primary and secondary streamers, and accelerated secondary streamer into stagnation. The repetitively pulsed breakdown is proceeded by the progressive axial prolongation of secondary streamers with bright heads and faint tails. Nonintuitively, the withstanding capability does not illustrate dramatic differences in dry air and humid air especially at high pulse repetition frequency. High-density residing hydrated ions with high electron bound energies (impeding streamer propagation) and the enhanced thermal release to cause higher reduced electric field (facilitating streamer propagation) may contrarily affect evolutions and discharge instability developments of positive streamer in humid air.

Supplementary material for this article is available online

Keywords: repetitively pulsed discharge, humidity, discharge instability, memory effect, streamer discharge

1. Introduction

Nanosecond repetitively pulsed (NRP) streamer discharges in open air have been demonstrated to enable versatile outcomes by flexibly gaining access to nonequilibrium chemistry, which is not available under thermal equilibrium or traditional slow-pulse excited conditions [1]. Wide-ranging applicability has been proved in plasma-assisted catalysis [2], plasma medicine [3], and plasma-assisted flow control [4].

The understanding and control of discharge instabilities under repetitive pulses are crucial for realistic applications to consistently produce reactive species within the long-term operation. For example, antitumor abscopal effects are induced by normal tissue irradiation using pulsed streamer plasmas in open air [3], where the spark breakdown is critically prohibited to prevent the thermal effect and the electric shock. Although in-depth discharge instability mechanisms have been proposed for the quasi-equilibrium [5] and radio-frequency plasmas [6], streamer discharges in open air excited by repetitive pulses experience complicated and sometimes unexpected unstable transitions (e.g. spark breakdown

* Authors to whom any correspondence should be addressed.

© 2023 IOP Publishing Ltd

[7], constrictions into highly ionized filaments [8, 9]). The streamer discharge is susceptible to environmental conditions (humidity, gas flow, etc) in open air [10, 11]. The gas humidity, either from the water vapor concentration in the surrounding air [12, 13] or intentionally supplemented in the gas inlet [14, 15], is an important factor for the plasma chemistry [16, 17]. On the other hand, streamer discharge evolutions under high-frequency repetitive pulses are more complicated than the conventional double-pulse test [18–20], e.g. the progressive spark formation [7], and periodical discharge regime transitions [18]. Discharge memory effects are generic concepts, however, relative contributions from different memory effect agents (residual charge, surplus heat, etc) are difficult to be quantitively determined [21]. Therefore, revealing streamer discharge instability mechanisms in humid air and under repetitively pulsed excitations is relevant for improving scaling-up capabilities and extending the applicability of plasma sources [22]. Note that the pulse-periodic streamer instability is not equivalent to dispersions of discharge inception or stochastics of streamer propagation.

Streamer properties are different in dry air and humid air:

(1) *Streamer discharge inception and propagation*. The corona pulse repetition frequency (PRF) under positive DC voltage in a corona cage increased with increasing the air humidity [23]. Streamer development would be hampered and the average critical electric field required for the gas gap breakdown (uniform electric field) increases with increasing the air humidity [24–26]. Electron swarm parameters, such as the electron energy distribution function, electron mobility, and electron diffusion coefficient, are dependent on the air humidity and the reduced electric field [27, 28]. Dissociative recombination of electrons with positive hydrated ions $H_3O^+(H_2O)_n$ and enhanced electron attachment to oxygen molecules are responsible for the decrease in the streamer channel conductivity [26].

(2) *Evolutions of dominant charged species in the afterglow period*. The ion hydration appears in humid air [29]. The reaction rate of three-body electron attachments of H_2O with O_2 is much bigger than that of O_2 [12, 13, 26]. Popov proposed that O_2^- ions rapidly transformed into ions with much bigger electron bound energies (e.g. O_3^-, NO_3^-) in dry air and hydrated ions (e.g. $O_2^-(H_2O)_n$, $NO_3^-(H_2O)_n$) in humid air [30]. The electron production efficiency in the streamer head would be reduced [30]. Starikovskiy *et al* systematically simulated streamer discharge in humid air and proposed that dominant positive ions in humid air are $H_3O^+(H_2O)_n$ [26]. The dominant positive ions experience the following scheme: $N_2^+ \rightarrow N_4^+ \rightarrow O_2^+(H_2O) \rightarrow H_3O^+(H_2O)_2 \rightarrow \ldots \rightarrow H_3O^+(H_2O)_n$.

(3) *Energy relaxation and thermal properties*. The local gas temperature rise is higher for a higher water concentration due to variations in energy relaxation schemes. Ono *et al* observed the temperature increase from 550 K to 850 K near the anode tip with the water vapor mole concentration increasing from 0.5% to 2.4% [31]. The enhanced temperature rise was also confirmed by temporally resolved Schlieren images and OH rotational temperature measurements [32, 33]. Komuro *et al* further explained the increase in the gas temperature based on rapid vibration-to-translation (V–T) transitions of H_2O and the exothermicity of the additional OH formation reactions [10]. Subsequent gas heating and gas expansion (potential causes of following streamer instabilities) were affected by accelerated vibrational relaxation via vibration-to-vibration (V–V) processes for O_2–H_2O and N_2–H_2O (time constants: 3 μs and 170 μs, respectively) [10]. Sainct *et al* measured the electron number density in NRP spark discharge in water vapor and found that 2% of water vapor was dissociated in the middle of the gap [34].

(4) *Breakdown voltage*. The breakdown voltage (uniform field) in humid air generally increases with increasing the air humidity [24]. Mikropoulos *et al* summarized that the time to breakdown decreased with increasing the air humidity [25].

The streamer discharge under single pulsed discharge and the post fast gas heating process have been simulated based on different models. Komuro and Ono established a two-dimensional fluid model for the atmospheric pressure streamer discharge in humid air and the internal molecular energy transfer was emphasized [10]. OH and NO temperature distributions and evolutions were discussed. The fast H_2O–H_2O V–T transitions and the enthalpy of OH formation reactions are the main causes of the additional gas temperature increase. Recently, Malagon-Romero *et al* simulated streamer propagation features, e.g. electron density, propagation velocity, electric field, in humid air based on a two-dimensional fluid model (*Afivo-streamer* framework) [13]. Higher humidity would lead to a thinner streamer body and slower propagation, which were attributed to the enhanced effective attachment rate. Another similar 2D axially symmetric fluid modeling of the streamer discharge in humid air was conducted by Starikovskiy *et al* with different gas pressures and water vapor contents [26]. The streamer development was hampered and the average critical electric field necessary for bridging the gas gap was increased in humid air. Evolutions of negative ion compositions after a pulsed streamer discharge in humid air were simulated by Popov based on a one-dimensional axisymmetric model [30]. Aleksandrov *et al* adopted a 1.5D model [35] and a 0D model [36] for discharge processes and species evolutions in dry and humid air. Temporal evolutions of densities of charged particles in the afterglow stage were obtained. Kinetics and important databases of charged species in non-equilibrium plasma in water vapor gaseous mixtures have also been comprehensively reviewed recently [17].

However, evolution characteristics and mechanisms of repetitively pulsed streamer discharge in humid air have not been sufficiently revealed yet. Contradictory contributions deserve further clarification for streamer evolutions. Specifically, on the one side, hydrated ions are with high electron bound energies but small mobilities. Whether these residing ions impede streamer propagations or provide abundant free electrons under following voltage pulses is required to be further revealed. On the other side, the enhanced thermal release in humid air induces higher *E*/*N* (reduced electric field), favorable for the streamer-to-spark transition under following voltage pulses. Evolutions of streamer dynamics under repetitive pulses in humid air affected by multiple memory effect agents are required to be determined. Repetitively pulsed streamer dynamics are probably different from those under the conventional 'double-pulse' method due to the integrated effect, e.g. accumulations and variations of residual charges and decays of thermal channels [37].

In this work, the experiment setup is briefly introduced in section 2. Streamer discharge characteristics are analyzed and compared for different air humidity conditions in section 3. Section 4 presents qualitative mechanisms and simulations of repetitively pulsed streamer discharge in humid air in terms of residual charge transport and energy relaxations.

2. Experiment setup

2.1. Experiment setup

Figure 1 schematically illustrates the experiment setup for repetitively pulsed streamer discharges in the dry and humid air. Electrical and optical diagnostics have been described in detail in our previous studies [18]. Pulsed high voltage and loop currents were measured by a commercially available voltage probe (Northstar Corp., PVM-5) and a current sensor (Pearson, Model 6585, 250 MHz), respectively. Emission light intensities from two selected spots (i.e. the needle tip and the middle gap, spot size: approximately 3 mm in diameter) were collected by two pairs of convex lenses and monitored by two photomultiplier (PMT) modules. Light intensity waveforms are registered by an oscilloscope (LeCroy Wavesurfer 10) in the sequence-resolved data logging mode. Therefore, electrical and optical waveforms in the same pulse train could be compared back and forth to obtain fundamental discharge parameters and their evolutions, such as the inception moment, average propagation velocity, and emission light rising slope. Besides, an intensified charge coupled device (ICCD) camera (PI-MAX4, 1024i) equipped with a UV lens (UV-100, 200–900 nm) was utilized to capture temporally resolved streamer images. It should be noted that ICCD images in section 3 are not captured under one voltage pulse due to the limited exposure capability. These ICCD images are selected from repeated tests (featuring similar emission light intensities and propagation positions) to demonstrate general evolutions of repetitively pulsed streamer discharges in humid air. Li *et al* demonstrated that the stroboscopic imaging technique was attractive with the ultra-high gating rate to track the ionization front propagation [38]. The combination of an intensifier and a high-speed camera would be implemented to reveal discharge evolutions in future investigations. The special double-image-feature (DIF) mode was utilized to obtain two images in quick succession to compare discharge trajectories between the primary streamer under the 2nd voltage pulse and the secondary streamer under the 1st voltage pulse in the same train. Furthermore, a z-type Schlieren system, consisting of a xenon lamp, a vertically aligned knife edge, and a high-speed camera (Phantom V2012, exposure rate: 160 kfps), was implemented to reveal gas density variations in the afterglow stage. The typical needle-plane electrode configuration was selected to generate the pulsed streamer discharge (needle tip radius: 100 μm, gap distance: 25 mm). The artificial air tank was utilized (80% N_2, 20% O_2). The preset maximum pulse number was 2×10^5 to reduce the experiment time consumption. Twenty repeated tests were conducted for each condition and the number of applied pulses before breakdown slightly varied at high PRF (depicted by error bars, standard deviations). Therefore, the number of applied pulses before breakdown under the same condition may be slightly different.

The air humidity was digitally controlled by changing percentages of the dry air (directly from the air tank) and the humidified air (through a water bubbler). The air humidity was measured by a commercial thermohydrometer (ColliHigh, JWSK-6, range: 5%–95%, accuracy: $\pm$3%) when the relative humidity (RH) was bigger than 5% or by a precious dew-point hygrometer (Vaisala DMT242, dewpoint temperature range: -60 °C–60 °C, accuracy: $\pm$2 °C) when the RH was smaller than 5%. The gas pressure inside the chamber was kept at 0.1 MPa, and no gas flow was present in current experiments. The ambient temperature remained at 20 °C. The absolute humidity was approximately 13.8 g m^{-3} when the RH was 80%. No condensation was observed. Most experiments were conducted in quiescent environment as benchmarks. Evolutions of repetitively pulsed streamer discharges under a transverse humidified air flow was investigated with a gas inlet near the gas gap (inlet port: outer diameter: 6 mm, inner diameter: 3.5 mm, distance to gap center: 40 mm, flow rate: 7.7 l min^{-1}).

2.2. 50% breakdown voltage under single pulse

Evolutions of repetitively pulsed streamer discharge are critically dependent on the applied voltage amplitude. 50% breakdown voltage under the single pulse ($U_{50\%}$) was first obtained based on the IEC standard. Detailed experiment procedure could be found in IEC 60060-1 (High-voltage test techniques-Part 1: General definitions and test requirements). Twenty breakdown events were selected to obtain $U_{50\%}$ in one up-and-down test (average value, under single pulse, voltage step: 1.5 kV, waiting period between two tests: 5 min). $U_{50\%}$ are important benchmarks for streamer evolutions under repetitive pulses. The repetitive working coefficient β_{rep} (<1) was defined as the ratio of the voltage amplitude of repetitive pulses to $U_{50\%}$ [39]. Further experiments on effects of the air humidity were conducted and compared based on the same β_{rep} ($\beta_{rep} = 0.7$).

The dependence of $U_{50\%}$ on RH is illustrated in figure 2. $U_{50\%}$ initially increases with increasing RH and reaches the peak approximately at 40%. $U_{50\%}$ then decreases and finally

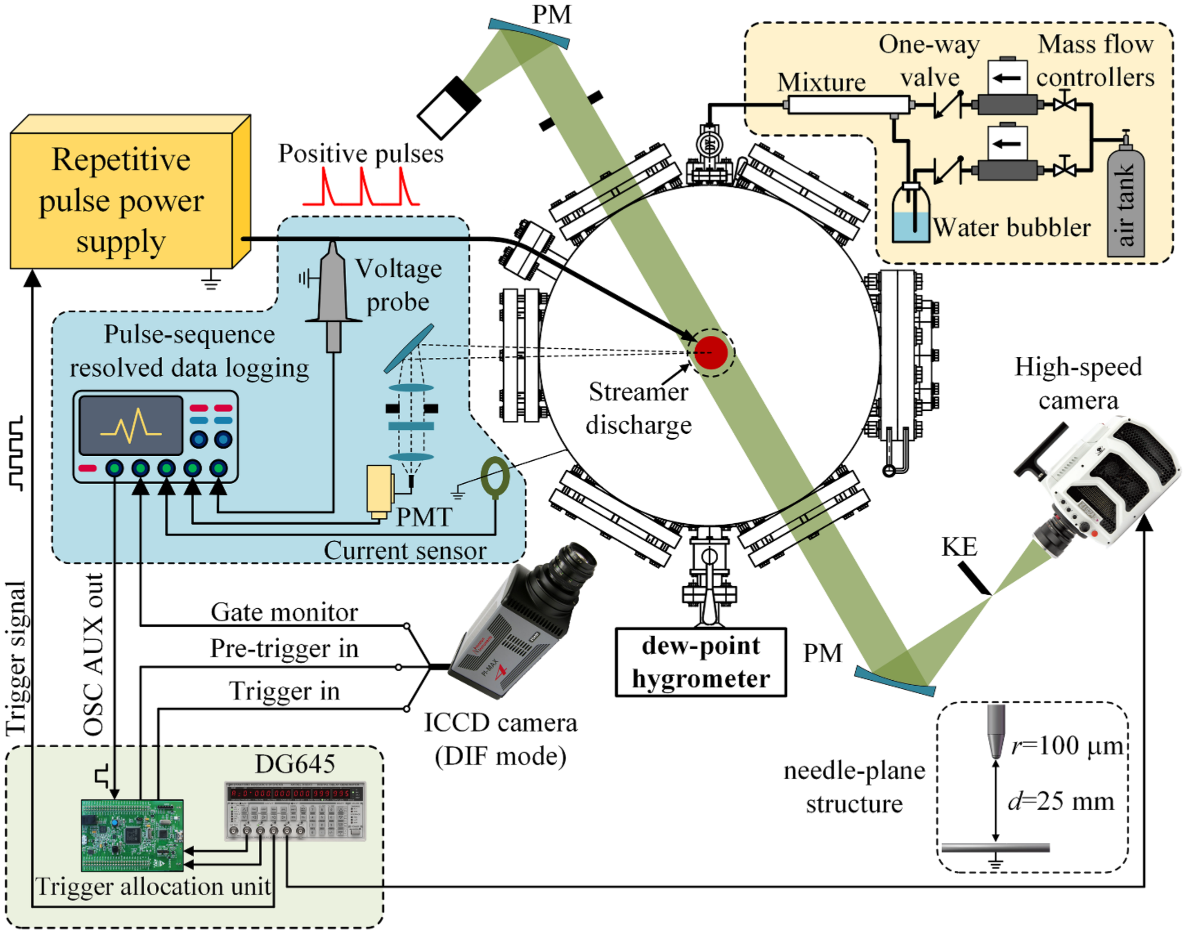

Figure 1. Schematic diagram of the repetitively pulsed streamer discharge in humid air. KE: knife edge, PM: Parabolic mirror. Two sets of PMT and lenses were utilized in the experiment. Cameras' positions are only schematically illustrated.

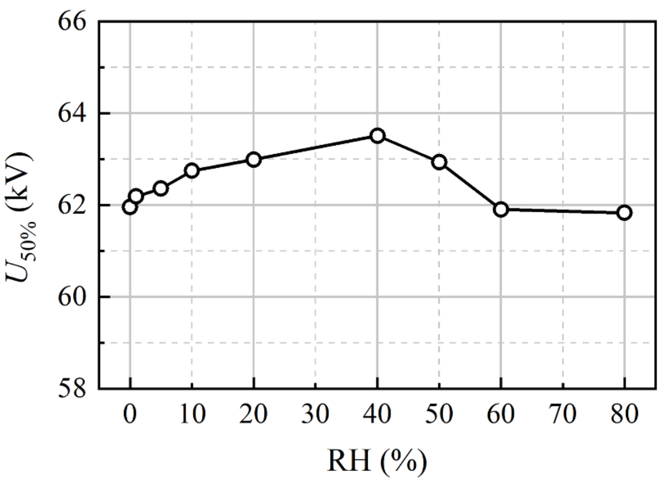

Figure 2. Effect of RH on the $U_{50\%}$ under single pulse in the needle-plane configuration.

saturates with further increasing RH. The increase in the breakdown voltage is conventionally explained in terms of the enhanced electron attachment in humid air. The 2nd decreasing stage is not consistent with monotonous breakdown curves in uniform fields under stationary AC or DC voltage.

3. Evolutions of repetitively pulsed streamer discharges in humid air

3.1. *Breakdown characteristics under repetitive pulses*

Dependences of the number of applied pulses before breakdown on the PRF and RH are illustrated and compared in figure 3. The breakdown curve in dry air has been discussed in our previous investigations [39], consisting of a fast-decreasing edge and a subsequent much flat tail with increasing PRF (i.e. an L-shaped curve). For discharges in humid air, breakdown curves have several similarities and differences:

(1) Low-PRF region. The number of applied pulses before breakdown exceeds the preset maximum pulse quantities in dry air and in RH = 20% and RH = 40% cases. Interestingly, breakdown curves resemble the capital Z (i.e. including three stages) for two high RH cases (RH = 60% and RH = 80%). For example, for RH = 60%, the number of applied pulses before breakdown remains around 2×10^3 from 100 Hz to 260 Hz, suggesting that the withstanding capability of the gas gap does not increase sharply in high air humidity scenarios compared with dry and low humidity cases. The discharge memory effect may persist for a longer period with increasing RH.

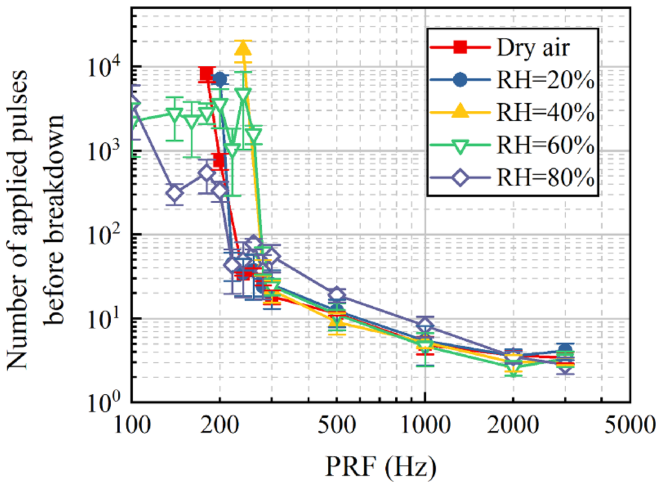

Figure 3. Dependences of the number of applied pulses before breakdown on PRF and RH ($\beta_{rep} = 0.7$, e.g. 43.3 kV in voltage amplitude for RH = 60%). The amplitude of repetitive pulses is dependent on $U_{50\%}$ at each RH, where β_{rep} is the same.

(2) Transition edges. The numbers of applied pulses before breakdown exhibit similar decreasing tendencies with increasing PRF, nevertheless, for RH = 20% and RH = 40%, the decreasing edges shift toward the high PRF side, indicating that the withstanding capability of the gas gap under repetitive pulses increases at medium PRF regions.
(3) High-PRF region. The numbers of applied pulses before breakdown are rather similar from 300 Hz to 3 kHz, indicating that the effect of air humidity on the insulation capability is not pronounced at high RPF. Unexpectedly, there are no dramatic differences in terms of the withstanding capability under high-PRF repetitive pulses in humid air compared with dry air, although the number of applied pulses before breakdown is significantly different in low-PRF region.

It is relevant to compare breakdown characteristics between humid air and N_2–O_2 mixtures due to the same trend of the enhanced electron attachment [15] but different photo-ionization capabilities. Similar variations of breakdown curves have been observed in N_2–O_2 mixtures compared with pure N_2 [40]. Nevertheless, the number of applied pulses before breakdown roughly linearly decreases with increasing PRF in the log-log plot for N_2–O_2 mixtures.

3.2. Benchmark: evolutions of streamer dynamics under repetitive pulses in dry air

Evolutions of streamer channels and the streamer-to-spark transition process at 2 kHz are illustrated in figure 4 in dry air as benchmarks for humid air. The ICCD exposure timings are indicated by grey boxes and the gate width is 5 ns. Conventionally, the pulsed streamer discharge has two stages, i.e. the primary streamer stage and the secondary streamer stage [41].

(1) Under the first voltage pulse, the primary streamer discharge exhibits the three-stage processes: 'inception cloud→shell formation→destabilization into filamentary channels' [20, 42, 43]. The secondary streamer does not fully reach the plane electrode in figure 4(a)-(4). The maximum radius of the shell R_{max} is as big as 9.8 mm under the very first voltage pulse. Meanwhile, the total number of filamentary channels is estimated no more than 6.
(2) Under the second voltage pulse, the inception moment and the morphology of the inception cloud are significantly different. The inception cloud is generated under a very low voltage (12.7 kV rather than 39.7 kV under the first voltage pulse). R_{max} is expected to fit with [43]

$$R_{max} = U/E_k \tag{1}$$

where U is the applied voltage to the electrode and E_k is the breakdown field. However, the diameter of the shell is too small to be identified. The quick filamentation process occurs after approximately only 10 ns as illustrated in figure 4(b)-(2). More than 15 filamentary channels are observed after the destabilization. The secondary streamers propagate towards the plane electrode in a more zigzag and slim manner than those under the first voltage pulse. Chen *et al* demonstrated that the number of break-up streamers was bigger with increasing PRF from 0.1 Hz to 10 Hz [20]. It was assumed that the more inhomogeneous background ionization at higher PRF created more streamers from the inception cloud, nevertheless, variations of streamer inceptions in the same pulse train had not been revealed in [20].
(3) The development into breakdown is characterized by the axial prolongation of secondary streamers of bright heads and faint tails in figure 4(c). The small shell formation and fast destabilization process are obvious. Meanwhile, the average propagation velocity of the primary streamer is faster than those under the previous two voltage pulses. The gas gap breakdown occurs at the pulse-falling edge. Interestingly, secondary streamer heads are much brighter than their tails, rather than straight ionization columns with uniform light emissions [41]. The radial region of the secondary streamer shrinks before the breakdown.

3.3. Evolutions of streamer dynamics under repetitive pulses in humid air: effects of air humidity

Evolutions of light intensities of streamer discharges under 2 kHz repetitive pulses are compared among three scenarios (dry air, RH = 20%, RH = 60%) in figure 5. Black, red, and blue curves represent the voltage waveform, light intensity around the needle tip, and light intensity at the middle gap, respectively. It should be noted that typical evolution features until breakdown are selected from repeated tests. Evolutions of light intensities under repetitive pulses before the gas gap breakdown are similar, including (1) the sharp rising edge under 1st voltage pulse, (2) a small spike before major light

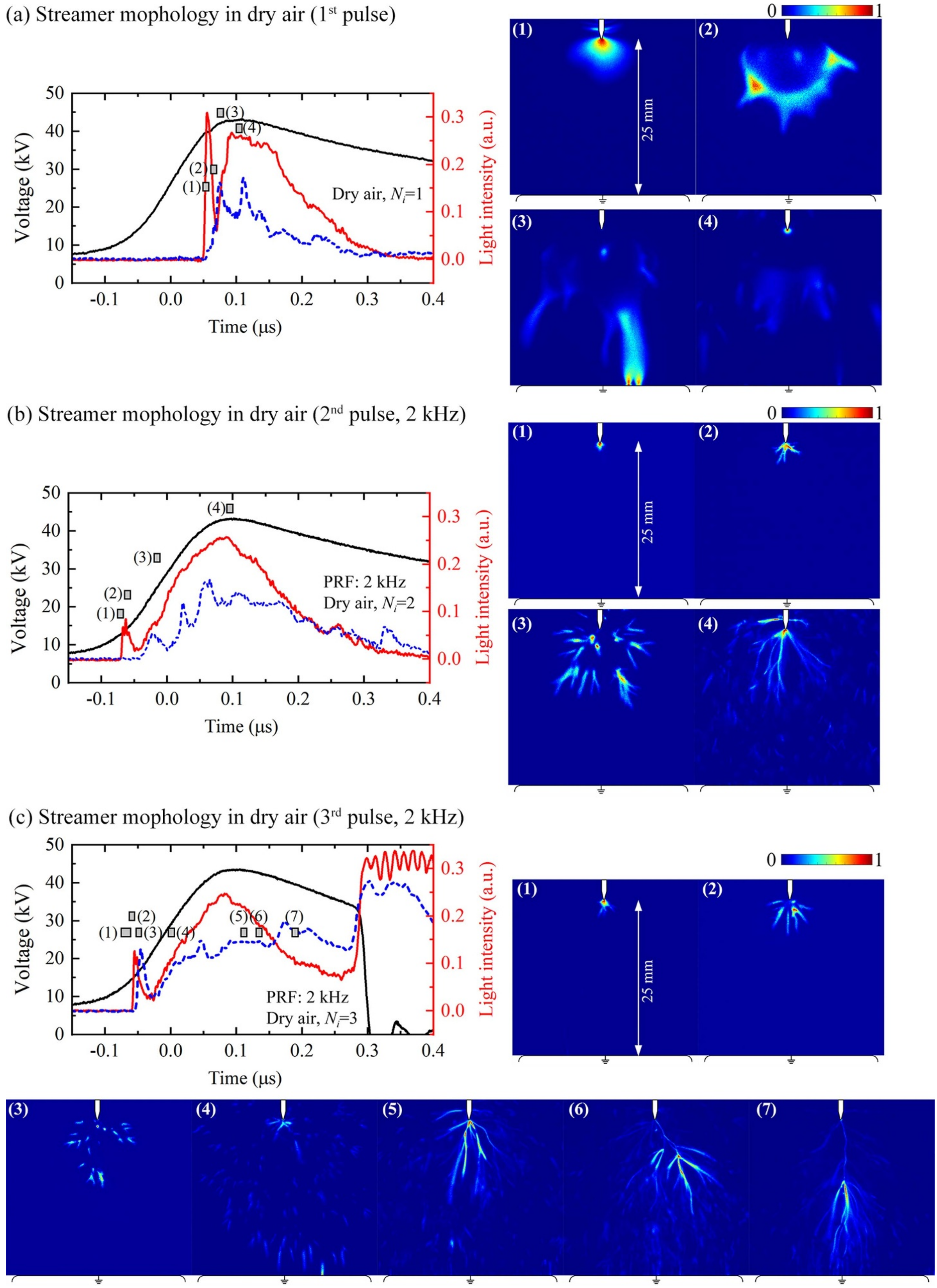

Figure 4. Evolutions of streamer channels under (a) 1st, (b) 2nd, and (c) 3rd voltage pulse at 2 kHz in dry air. Images are selected from independent tests featuring similar emission light intensities.

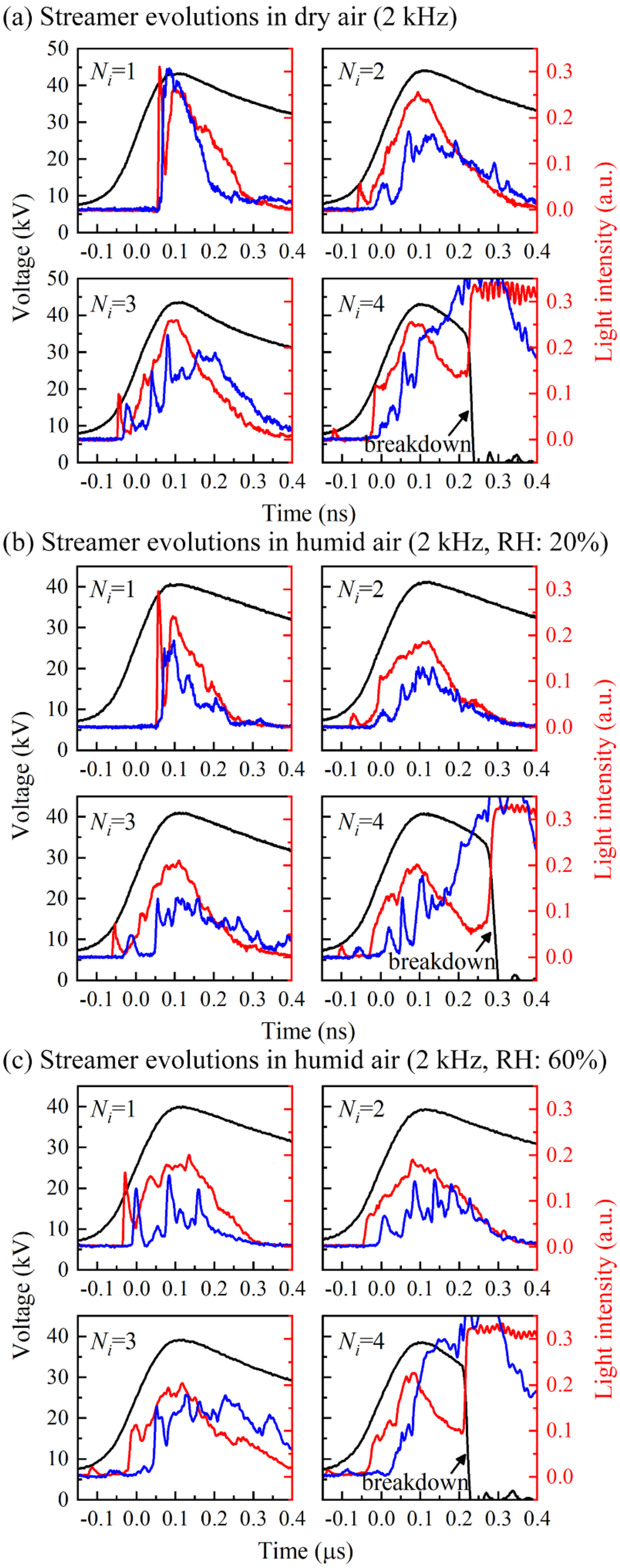

Figure 5. Evolutions of light intensities before breakdown in dry air and humid air (RH = 20% and RH = 60%). β_{rep} is 0.7 in each scenario. Black, red, and blue curves represent the voltage waveform, light intensity around the needle tip, and light intensity from the middle gap, respectively.

intensity rise under 2nd voltage pulse, and (3) earlier streamer inception under following voltage pulses, (4) slower average primary streamer propagation velocity (inferred from the time delay between two light intensity waveforms' fronts) under following voltage pulses. Nevertheless, distinct propagation features are identified with increasing the air humidity.

(1) Under the first voltage pulse, both the amplitude and inception moment of the emission light intensity around the needle tip and at the middle gap are lower with increasing RH. Meanwhile, the average propagation velocity of the primary streamer decreases with increasing RH, possibly related to the earlier inception and the enhanced electron attachment. Starikovskiy *et al* found that the streamer propagation velocity dramatically decreased with even increasing the water concentration to 1% (absolute humidity) [26]. For a fixed voltage amplitude, the positive streamer failed to reach the opposite electrode for 3% (absolute humidity).
(2) Under the second voltage pulse, the inception moment of the small light spike before the major rising edge decreases with increasing RH (the earliest small light spike is beyond the x-range for RH = 60%). The small light spike, occurring under a very low voltage amplitude, is generated by the weakly ionized region around the needle tip. This phenomenon is probably caused by abundant residual electron sources around the needle tip. Meanwhile, oscillations of the light intensity at the middle gap are more intense for higher RHs. This feature indicates that more streamer filaments propagate through the viewing pyramid of the PMT module.
(3) Before the gap breakdown, although most appearances of light intensity waveforms are similar, the rising edge of the light intensity at the middle gap is smoother for higher RH (RH = 60%) than that in dry air.

Note that the gas gap breakdown under 4th voltage pulse in figure 5(a) rather than under 3rd voltage pulse in figure 4(a) is due to slight variations in the number of applied pulses test-by-test.

Effects of the presence of water vapor on evolutions of pulse-periodic streamer discharges are illustrated in figure 6. Several differences in terms of streamer evolutions are identified in humid air.

(1) A much smaller inception cloud and more numbers of filamentary streamer channels under the first voltage pulse. In figure 6(a)-(1), the diameter of the inception cloud is approximately 1.4 mm, only 55% of that in dry air. Although the streamer inception moment is much earlier than that in dry air, the number of filamentary streamer channels with bright heads is significantly increased by 80%. This feature may suggest that the enhanced electronegativity from water vapor causes more stochastics to

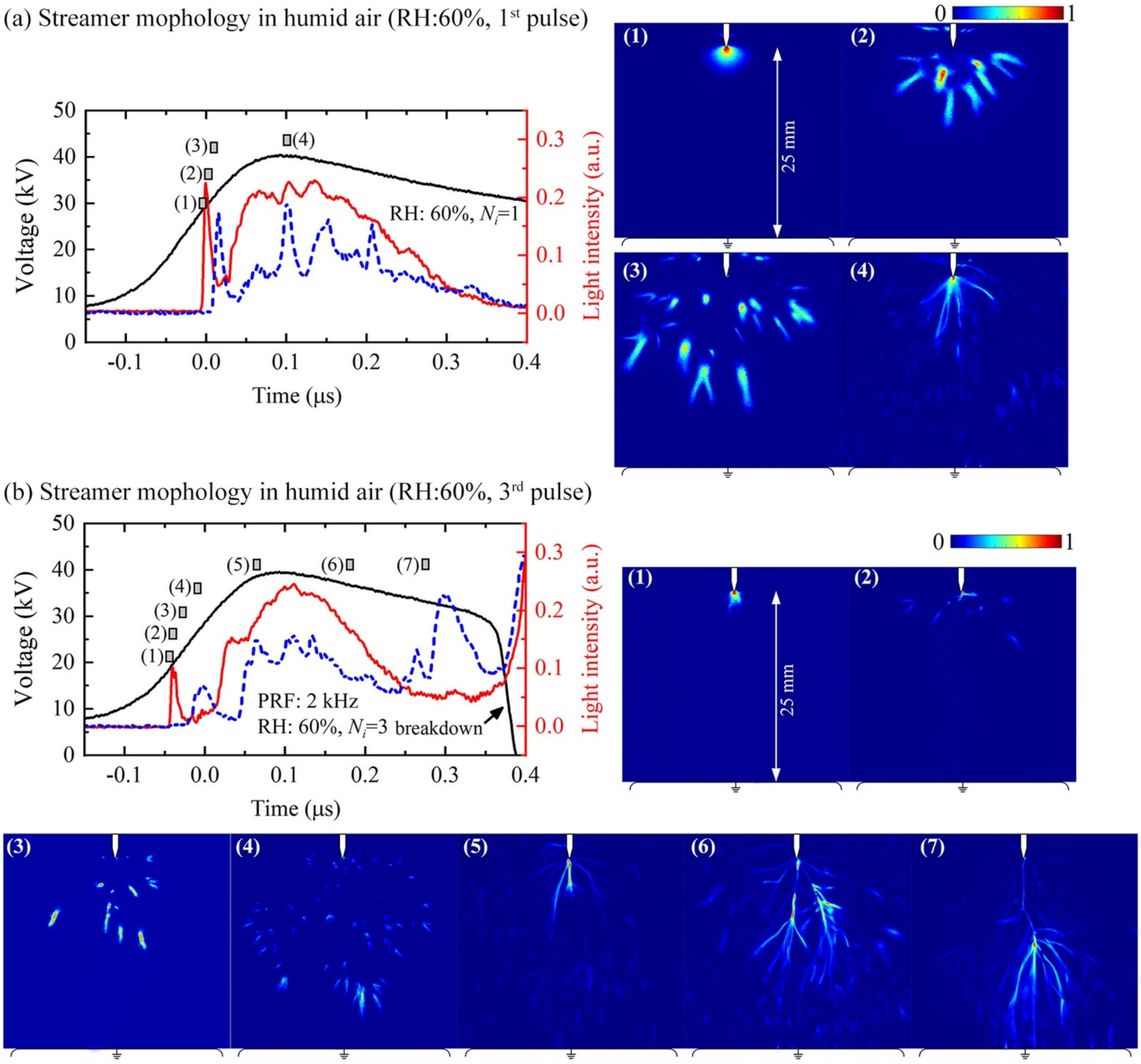

Figure 6. Evolutions of streamer channels under 2 kHz repetitive pulses until breakdown in humid air (RH = 60%). (a) Under the first voltage pulse. (b) Under the second voltage pulse. The ICCD exposure timings are indicated by grey boxes and the gate width is 5 ns in each image. The secondary streamer image is enlarged before breakdown.

the streamer filamentation since free electron sources in front of the streamer head are critical for positive streamers. The maximum radius of the shell before destabilization is estimated as 5.1 mm, only 52% of that in dry air. The increase of the critical breakdown field in humid air based on previous experiments in uniform electric fields could be estimated as 4% [44]. $R_{\max}$ is scaled down because the voltage amplitude is reduced (approximately by 25%) and the critical breakdown field is increased. Nevertheless, $R_{\max}$ does not strictly follow the formula (1). The shell formation has not been captured probably due to the fast destabilization process.

(2) More radial expansion and branches before the secondary streamer touches the cathode. The streamer branching is more pronounced in humid air (RH = 60%). For example, more than three bright branches originate from the same root in figures 6(b)-(7) and (b)-(8). On the contrary, in dry air, only one or two bright streamer channels propagate towards the plane electrodes in figures 4(b)-(7) and (b)-(8). This difference may suggest that there are more ionization sources in humid air under repetitive pulses. However, the instantaneous diameter of the secondary streamer is roughly identical in dry air and in humid air.

3.4. Evolutions of streamer dynamics under repetitive pulses in humid air: effects of PRF

The discharge memory effects are originated by residuals of longer decay timescales than the ‘pulse-off’ period. Effects of PRF are of critical importance for streamer dynamics under repetitive pulses. The dependences of light intensities on PRF in humid air (RH = 20%) are illustrated in figure 7. The light intensities under the second voltage pulse dramatically change with decreasing PRF from 3 kHz to 300 Hz. Under 3 kHz repetitive pulses, the light intensity around the needle tip under the second voltage pulse is significantly lower than

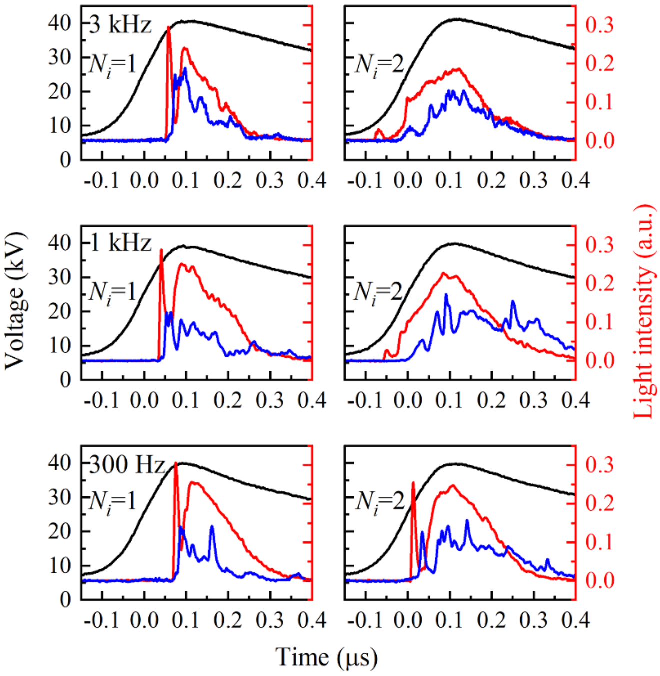

Figure 7. Effects of PRF on light intensities of streamer discharges in a pulse train (RH = 20%).

that under the very first one. Under 300 Hz repetitive pulses, the above tendency is not obvious. Besides, the pulse width of the light intensity waveform consistently grows bigger under the second voltage, which suggests that the streamer discharge persists for longer periods.

Effects of PRF on evolutions of streamer channels in humid air are illustrated in figure 8. Previous studies mainly emphasize the effect of PRF on streamer morphology in a steady state [20]. In the double-pulse test of positive streamer dynamics, streamer channel images under two voltage pulses were superimposed to visualize channel variations [19]. However, streamer evolutions under following voltage pulses in humid air have not been adequately discussed yet. Important differences between streamer evolutions at 100 Hz and 2 kHz are summarized as follows.

(1) The smaller inception cloud and the earlier break-up are identified during the primary streamer inception and propagation. Nijdam *et al* also observed that the size of the inception cloud in 200 mbar air decreased with increasing PRF from 0.01 Hz to 10 Hz [19]. It was proposed that the apparent paradox had not been well resolved because smoother distributions of residual charges at higher PRF may be favorable for a larger inception cloud rather than facilitating the earlier break-up [19].
(2) The average propagation velocity at 2 kHz is higher than 100 Hz inferred from a shorter time delay between two light intensity rising edges.
(3) The estimated diameter of the secondary streamer under the 2nd voltage pulse is 0.37 mm at 100 Hz and 0.27 mm at 2 kHz, respectively. The electric field in front of the positive streamer head may be more intensified at 2 kHz due to a smaller streamer diameter. Consequently, the final streamer-to-spark transition may be triggered at higher PRF.

3.5. Evolutions of streamer dynamics under repetitive pulses in humid air: effects of transverse gas flow

The residual charge transports and decay of thermal channels are accelerated by the additional gas flow, consequently, the repetitively pulsed streamer discharges may be different. The mean number of applied pulses before breakdown with the transverse gas flow is 2 at 2 kHz, which is close to the scenario without the gas flow. Effects of the transverse gas flow on streamer dynamics under repetitive pulses in humid air (RH = 60%) have been determined and illustrated in figure 9 (air flows from the right-side to the left-side). The total inlet air was 7.7 l min^{-1}, and the gas pressure remained at 0.1 MPa through a needle valve at the chamber outlet. Meanwhile, the primary streamer resembles those without the transverse gas flow. However, the secondary streamer propagation is different with the transverse gas flow. The most pronounced difference is that the secondary streamer channel has less branches with the presence of transverse air flow compared with figure 6(b). The diameter of the secondary streamer decreases to approximately 0.18 mm. The measured gas flow velocity is 2.7 m s^{-1} near the needle tip by a hot-wire gas velocity meter (Fluke F923). The gas movement distance is calculated as 1.35 mm with a 500 μs pulse-off period (2 kHz), which is eight times bigger than the secondary streamer diameter. Therefore, the removal of residual hydrated ions in the gas gap may reduce discharge stochastics of the secondary streamer, meanwhile, the less availability of free electrons leads to a thinner streamer body.

3.6. Following phenomena of streamer channels under repetitive pulses

The following tendency of streamer channels is an important memory effect phenomenon under repetitive pulses, which would cause the lateral narrowing of discharge regions and the final breakdown. Therefore, effects of the previous secondary streamer on the subsequent primary streamer are particularly determined because leftovers are critical for following breakups from the inception shell.

Streamer channel variations in dry air and humid air under consecutive two voltage pulses are obtained. The propagation trajectories of the primary streamer under the 2nd voltage pulse are correlated with those of the secondary streamer under the 1st voltage pulse in the same pulse train. This correlation is enabled by the DIF mode of the ICCD camera (interline CCD operation), where two images with different exposure timings

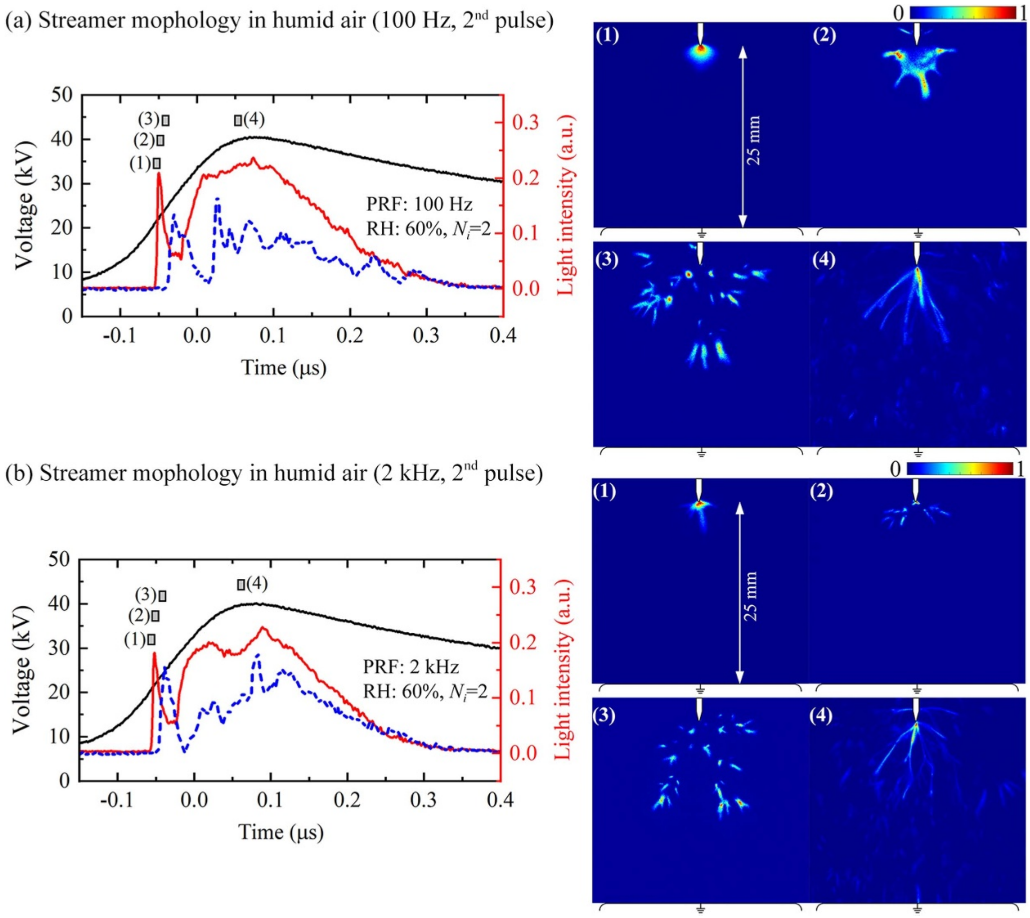

Figure 8. Effect of PRF on evolutions of streamer channels in humid air (RH = 60%). Note that no gas gap breakdown occurred under the second voltage pules in both scenarios.

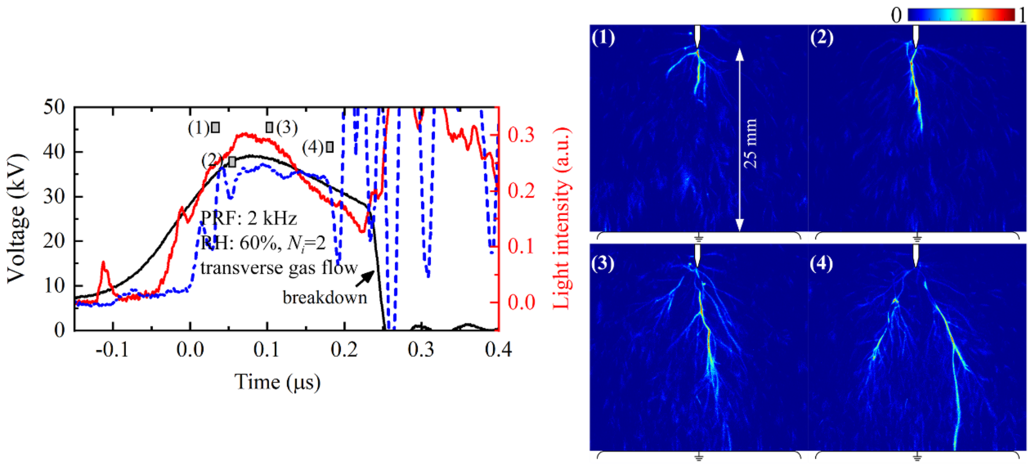

Figure 9. Secondary streamer development under the second pulse in transverse air flow (RH = 60%, gas flow rate: 7.7 l min^{-1}, PRF: 2 kHz).

are captured in quick succession. In this special operation, the first exposure slot is on the secondary streamer stage under the 1st voltage pulse, while, the second exposure slot shifts to the primary streamer stage under the 2nd voltage pulse in the same pulse train. Less than 30% residual images inevitably exist in the second image at 1 kHz due to the relatively long phosphor decay time (P43 plane: ∼1 ms). However, they are distinguishable in the second image. Several distinct discharge channel following phenomenon in dry and humid air are summarized in figure 10:

(1) In dry air, the primary streamer under the 2nd voltage pulse does not illustrate apparent preferences (only 3 out of 8 channels) to the previous secondary streamer trails (depicted by white dashed lines) for the very first two voltage pulses.
(2) In contrast to the dry air, significant channel following tendencies have already appeared in the first discharge pair (5 out of 6 channels) in humid air (RH = 60%). This tendency suggests that the next primary streamer prefers to propagate inside 'old trails'. Following tendencies of the primary streamer are only slightly weakened by reducing PRF to 100 Hz in humid air. The above observations prove that discharge memory effects in humid air are more pronounced.
(3) The channel following phenomena are clearer in subsequent discharge pairs. More than half of primary streamers under 3rd voltage pulse follow secondary streamer trajectories under 2nd voltage pulse in dry air (not shown here).

Two new parameters are proposed to characterize the discharge following phenomenon. Table 1 summarizes the probability of occurrence (P_1) of the primary streamer following phenomena in repeated tests and the average percentage of primary streamer heads propagating inside 'old trails' (P_2) based on ICCD images. P_1 is defined as the ratio of the number of tests with the primary streamer following phenomenon to the total number of tests (20 in present experiments). The discharge following phenomenon refers to the scenario when at least one primary streamer channel head under $(N_i + 1)^{\text{th}}$ voltage pulse clearly followed the previous secondary channels under N_i^{th} voltage pulse. For example, P_1 is 0.5 if the primary streamer following phenomenon is observed in 10 tests. P_2 is proposed as the ratio of the number of primary streamer heads propagating inside 'old trails' to the total number of primary streamer channels in a specific test when the primary streamer following phenomenon appears. For example, there are 6 primary streamer channels under the 2nd voltage pulse in figure 10(b)-(3), among which 5 channels follow the secondary streamer trajectories under 1st voltage pulse (denoted by white dashed lines), then, P_2 is 0.83. From discharge statistics in table 1, P_1 and P_2 are generally bigger in humid air and under following discharge pairs, suggesting the primary streamer is more prone to be attracted by old trails in humid air. The effect of PRF on the primary streamer following phenomenon is more pronounced for the first three pulsed discharges in humid air than dry air. Nijdam *et al* found that the second streamer still occupied many regions of the old channels at 1 ms pulse-to-pulse interval in 133 mbar air [19], similarly, in present investigations, streamer channels follow previous trails at 1 kHz in humid air. It should be noted that the misjudgment of channel overlapping may be due to the projection of 3D streamer filaments into a 2D image plane. Nevertheless, pronounced effects of air humidity and PRF on the following phenomena of streamer channels could be supported by current results.

Schlieren images in a 2 kHz pulse train are compared between humid air (RH = 60%) and dry air in figure 11. The

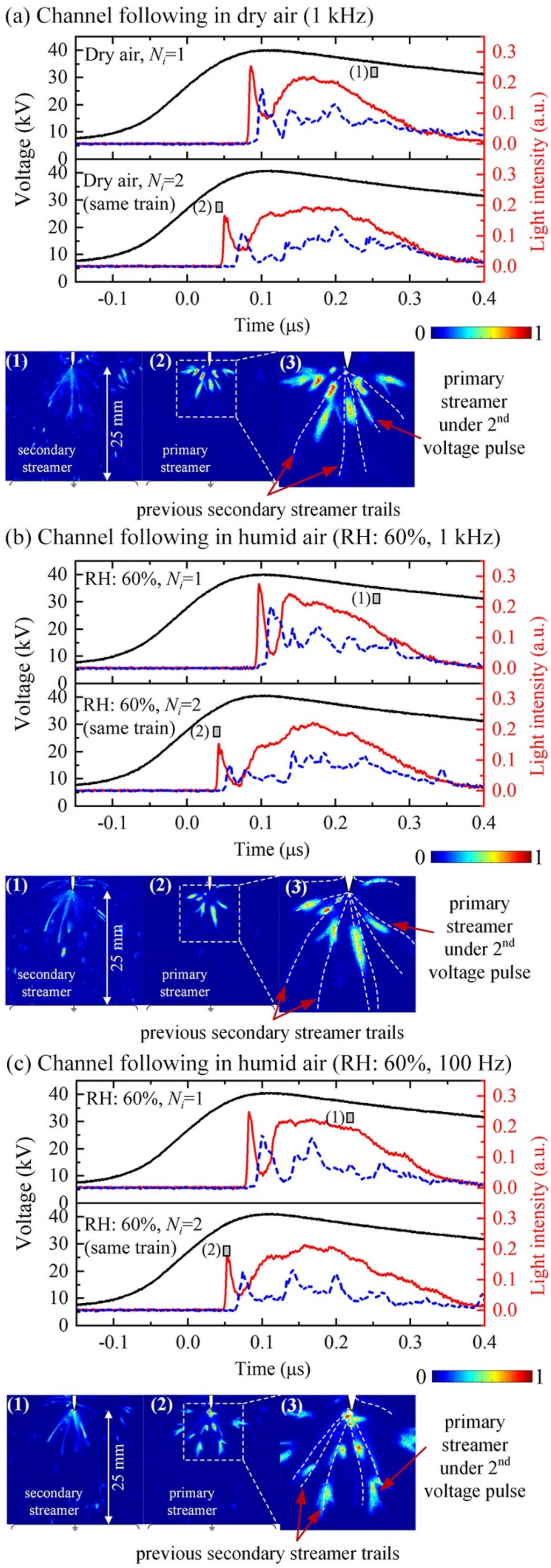

Figure 10. Channel following phenomena under repetitive pulses in (a) dry air, 1 kHz, (b) humid air, RH = 60%, 1 kHz, and (c) humid air, RH = 60%, 100 Hz in the same pulse train. Previous secondary streamer trails are indicated by white dashed lines.

Table 1. Comparisons on probability of occurrence (P_1) of the following phenomena in repeated 20 tests and the percentage of primary streamer heads propagating inside 'old trails' (P_2) in humid/dry air and different PRF.

Discharge condition	1 kHz, 2nd/1st pulses		1 kHz, 3rd/2nd pulses		100 Hz, 2nd/1st pulses		100 Hz, 3rd/2nd pulses	
	P_1	P_2	P_1	P_2	P_1	P_2	P_1	P_2
Dry air	0.20	0.40 ± 0.08	0.58	0.65 ± 0.10	0.23	0.5 ± 0.09	0.53	0.59 ± 0.14
Humid air (RH = 60%)	0.46	0.68 ± 0.14	1	0.71 ± 0.15	0.66	0.59 ± 0.05	1	0.55 ± 0.17

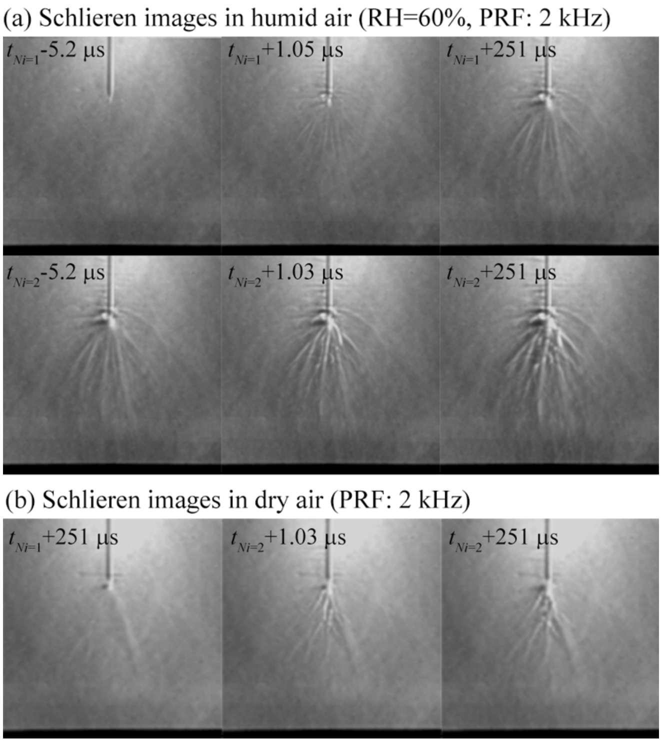

Figure 11. Schlieren images in a 2 kHz pulse train in (a) humid air and in (b) dry air. $t_{Ni=1}$ and $t_{Ni=2}$ represent the 1st and 2nd streamer inception moments, respectively ($t_{Ni=2} - t_{Ni=1} \approx 500$ μs). The imaging area was cropped to increase the sample rate to 160 kfps (6.24 μs time delay between two images and 1 μs exposure time for each image).

post-discharge heated channel is more pronounced in humid air than in dry air. The full diffusion time of heated channels is approximately 29.6 ms for humid air (RH = 60%), while, 22.7 ms for dry air by comparing Schlieren images back and forth (captured by a high-speed camera). In humid air, the similar following phenomena of illuminating streamer channels are applicable for heated areas, which implies that the high gas temperature inside previous trails would attract following streamers and facilitate their propagations towards the plane electrode. Higher deposited energies in humid air under following voltage pulses cause more intensive heat release (see supplementary file). In dry air, the deposited energy was approximately 6.3 mJ for the first streamer discharge and 4.53 mJ for the second streamer discharge. The decrease in the deposited energy under following voltage pulse is probably related to the higher pre-ionization level [45, 46]. Nemschokmichal *et al* proved that a larger pre-ionization level would lead to a lower breakdown voltage, an earlier discharge ignition, and a lower current pulse maximum [45]. Nevertheless, in humid air (RH = 60%), the deposited energy was calculated as 5.7 mJ for the first streamer discharge and 6.48 mJ for the second streamer discharge. This increasing trend is probably related to: (1) a much lower electron level with the presence of H_2O molecule, and (2) a higher reduced electric field due to the enhanced thermal release. Similar discharge energy evolution trend is also observed in flowing dry and humid air, nevertheless, the deposited energy is higher with the transverse gas flow possibly due to removals of residual charges and heat.

4. Discussions

4.1. Simulations of streamer dynamics and species evolutions in humid air

Residual charge transport and energy relaxation, two fundamental processes in terms of discharge memory effect mechanisms under repetitive pulses, are difficult to determine directly from experimental observations. These two processes are dramatically different when the water vapor is present. In humid air, the discharge memory effect may originate from not only residual charges that provide excessive free electrons but also surplus heat that leads to an increase in E/N.

Evolutions of streamer dynamics in humid air under pulsed voltage are simulated using a 2D–0D combined approach (*Afivo-streamer* framework + *ZDPlasKin* code). Simulation setups are described in the appendix. Chen *et al* implemented a similar approach to reveal streamer-to-spark transitions in the first pulse and the post discharge stage (*PASSKEy* code+ *ZDPlasKin* code) [47]. Note that the preliminary simulation, including one pulsed streamer discharge and one afterglow stage, is to qualitatively explain evolution tendencies observed in experiments. The streamer-to-spark transition and the possible spark-to-thermal channel transition are extremely complicated [47, 48] and are out of the scope of the present investigation. Besides, the streamer-to-spark transition may occur after several voltage pulses at high PRF and even several thousand voltage pulses at low PRF. The continuous simulations of long-term repetitively pulsed discharge require precious distributions of various memory effect agents. Evolutions and propagation patterns of secondary streamers are affected by the air humidity in figure 12. Meanwhile, the streamer propagation at elevated temperature (400 K) and

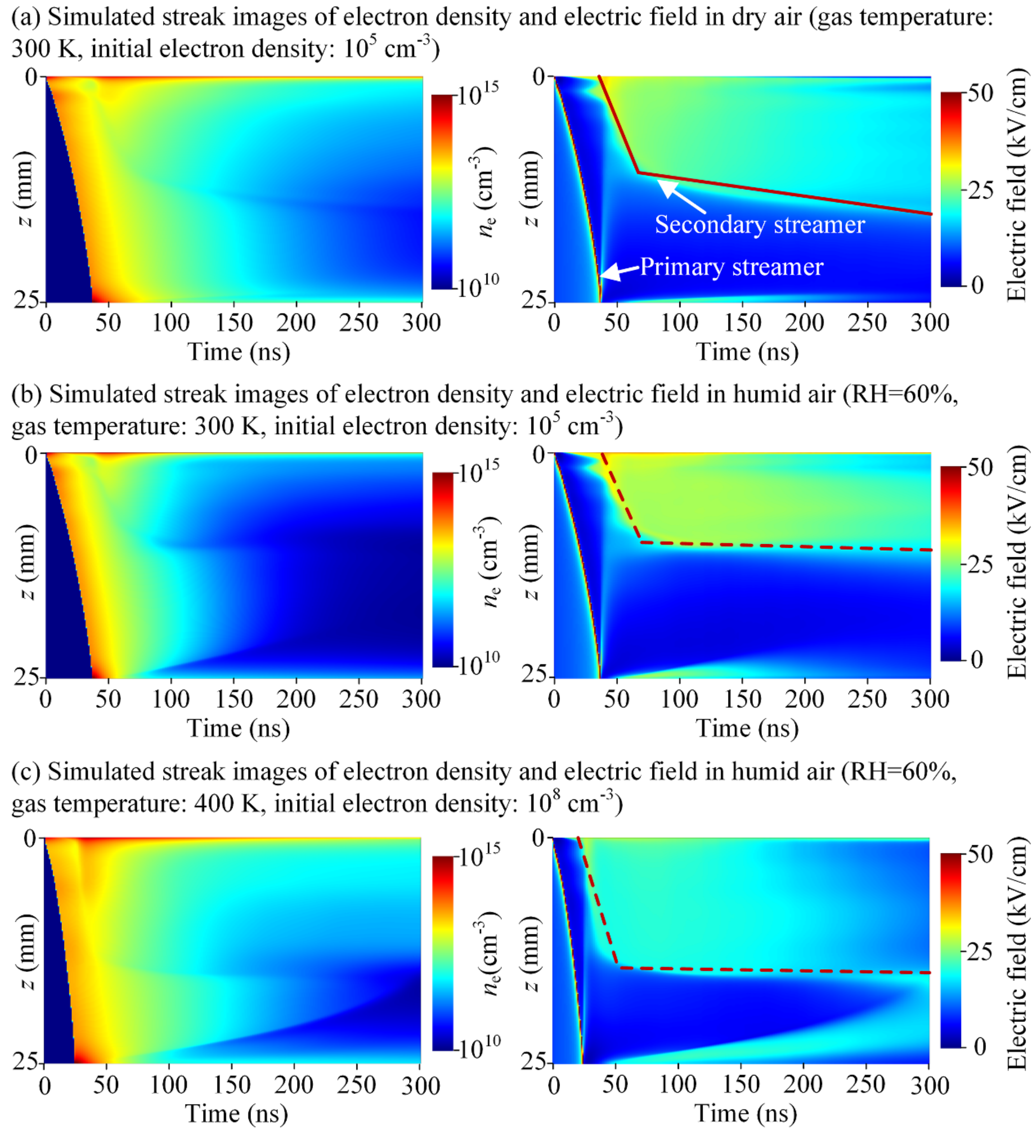

Figure 12. Simulated streak images along the axis for electron density (left column) and electric field (right column) in (a) dry air, gas temperature: 300 K, initial electron density: 10^5 cm^{-3}, (b) humid air, RH = 60%, gas temperature: 300 K, initial electron density: 10^5 cm^{-3}, and (c) humid air, RH = 60%, gas temperature: 400 K, initial electron density: 10^8 cm^{-3}. Solid and dashed red lines depict development stages of the secondary streamers in dry air and humid air, respectively.

higher initial electron density (10^8 cm^{-3}) is also compared. The simulated temperature is a rough estimation of the gas temperature [33]. In dry air, the development of a secondary streamer has three stages, i.e. the first fast expansion stage (average velocity: 0.34 mm ns^{-1}), the following slow propagation stage (average velocity: 0.02 mm ns^{-1}), and the stagnation stage (not shown here). In contrast, only the first fast expansion stage and the stagnation stage exist in humid air (RH = 60%), suggesting a faster formation of the secondary streamer. The formation of the secondary streamer is traditionally described by the attachment instability criteria [49], where the plateau region with a high electric field is referred to as the secondary streamer. The electric field distribution in the secondary streamer channel is inversely proportional to the channel conductivity σ_{ss}

$$\sigma_{ss} = e n_e \mu_e \tag{2}$$

where e, n_e, and μ_e are elementary charge, electron density, and electron mobility, respectively. The exponential decay of the electron density could be expressed as

$$n_e = n_{e0} \exp(-A_a t) \tag{3}$$

where n_{e0} and A_a are the initial electron density and the net electron attachment frequency, respectively. Bigger A_a in humid air would lead to faster channel conductivity decay. Since the formation of the secondary streamer region is governed by depletions of free electrons and the electric field rise according to the attachment instability criteria [49], enhanced net electron attachments in humid air would accelerate the formation of a secondary streamer. Therefore, the slow

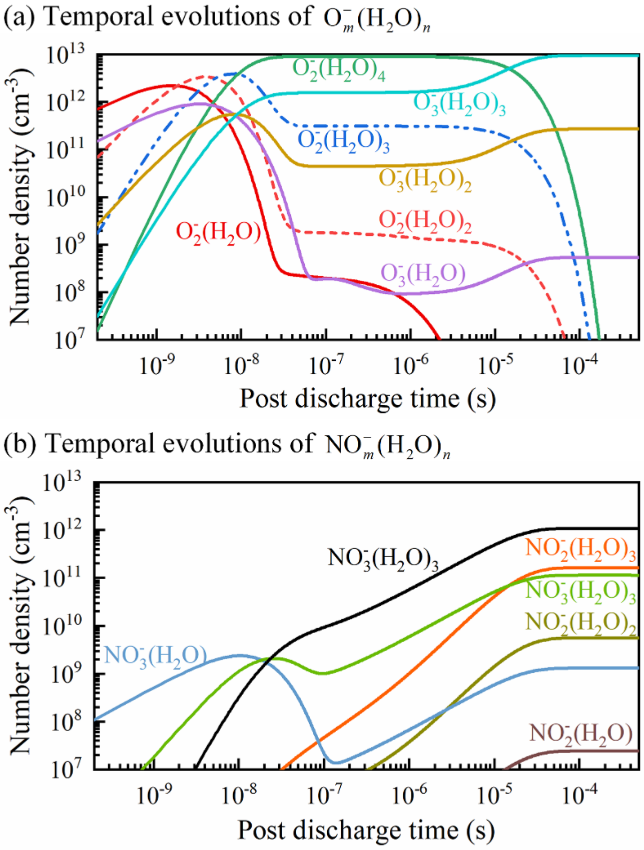

Figure 13. Temporal evolutions of (a) $O_m^-(H_2O)_n$ and (b) $NO_m^-(H_2O)_n$ in humid air (RH = 60%) during the post discharge stage. The gas temperate remains at 300 K.

propagation stage may disappear and the stagnation stage is earlier in humid air. The length of the secondary streamer is longer at elevated temperature and higher initial electron density in figure 12(c) as expected. Meanwhile, the electric field inside the secondary streamer region is generally lower and the high electric field region expands from the cathode. The electron attachment coefficient is lower at elevated temperature and then the electric field decreases due to higher free electron density. Consequently, the electric field between the secondary streamer column and the plane electrode may grow.

Charged species decay within the 'pulse-off' period determines the initial conditions under the following voltage pulses. Ion-ion recombination processes are mainly included in the present global model. In dry air, major negative ions are O_3^-, O_2^- and O_4^- at the end moment of the 2D model. The density of O_3^- decreases by two orders of magnitude (to 10^{10} cm^{-3}), and the densities of O_2^-, O_4^-, and NO_3^- decrease to 10^9 cm^{-3} after 500 μs. However, negative ion compositions and conversions are rather complicated in humid air due to the formation of hydrated ions, which affects free electron productions under following voltage pulses. Figure 13 demonstrates temporal evolutions of major negative ions. The presence of H_2O leads to the rapid hydration of negative ions and eventually, the dominant negative ions are $O_3^-(H_2O)_n$ and $NO_3^-(H_2O)_n$ with maximum $n = 3$ in present and other similar models [13, 50]. The density of $O_3^-(H_2O)_3$ remains as 10^{13} cm^{-3}, and $NO_3^-(H_2O)_3$ is 10^{12} cm^{-3}. Because electron affinities of hydrated clusters $NO_3^-(H_2O)_n$ (3.9 eV–4.9 eV for $n = 0$–2) and $O_3^-(H_2O)_n$ (1.89 eV–2.86 eV for $n = 0$–2) are much bigger than O_2^- (0.44 eV) in dry air [43], the production rates of free electron in the streamer head in humid air by the detachment of hydrated negative ions are probably much lower despite of their high number densities. Although the long lifetime and high number density of negative ions in humid air reside in the gas gap, they may not facilitate (impede instead compared with dry air) the development of positive streamers under repetitive pulses as intuitively expected.

Most simulation works regarding streamer discharge in humid air implement 2D fluid models to reveal general streamer propagation features and effects of the air humidity. The full validation of repetitively pulsed streamer discharge is extremely difficult, e.g. the clear branching feature of the positive streamer channel, and pronounced gas heating in the afterglow stage. The *Afivo-streamer* framework is implemented to simulate the pulsed streamer discharge, which has been validated by comparing simulation and experiment results in a previous investigation [51]. Streamer velocities, radii, and light emission profiles were compared both qualitatively and quantitatively, where the streamer discharge was produced at low air pressure (0.1 bar) to ensure reproductivity [51]. The same validation was also emphasized by Ono and Komuro [41], where the single-filament pulsed positive streamer discharge was produced in a specialized electrode system. Therefore, the main purpose of the present preliminary simulation is to qualitatively explain experimental evolution tendencies. Several selected parameters are compared between experimental observations and simulation results in terms of pulsed streamer propagations. It should be noted that the branching feature could not be incorporated in present simulations, although it may be affected by the air humidity as illustrated in figure 6.

(1) Channel diameter. In experiments, the measured primary streamer channel diameter is approximately 0.94 mm when the primary streamer head propagates to the middle position of the gas gap in humid air (RH = 60%). The simulated streamer channel diameter is 1.0 mm (300 K, initial electron density: 10^5 cm^{-3}) and 1.4 mm (400 K, initial electron density: 10^8 cm^{-3}), respectively, when the streamer head reaches the middle gap in humid air (RH = 60%).
(2) Propagation velocity. The average propagation velocity of the primary streamer could be estimated as 0.58 mm ns^{-1} from the time delay between two light intensities in humid air (RH = 60%). In simulations, the average propagation velocity is 0.54 mm ns^{-1} (300 K, initial electron density: 10^5 cm^{-3}) and 0.78 mm ns^{-1} (400 K, initial electron density: 10^8 cm^{-3}), respectively, when the streamer head reaches the middle gap in humid air (RH = 60%).

Note that the difference in the development stages of the secondary streamer illustrated in figure 12 has not been visualized yet by the present ICCD camera due to the limited

Table 2. Summary on microscopic and macroscopic effects of the air humidity on repetitively pulsed streamer discharges.

Microscopic variations of streamer discharge in humid air from literatures	
(a) Electron attachment	6–10 times bigger with H_2O than O_2 [13]
(b) Electron detachment	Inhibited, delaying the occurrence of seed electrons [30]
(b) Electron swarm parameters	Mobility and diffusion coefficients dependent on *E*/*N* [27]
(c) Photoionization	Negligible due to $k_{O2}\cdot n[O_2] \gg k_{H2O}\cdot n[H_2O]$, *n*: number density *k:* absorption coefficient [26], reduce the UV absorption length
(d) Evolutions of charged species	Positive ions: $H_3O^+(H_2O)_n$ clusters in humid air [26] Negative ions: hydrated ions (e.g. $O_2^-(H_2O)_n$, $NO_3^-3(H_2O)_n$) [30]
(e) Discharge current	Decrease by several orders of magnitude with 3% H_2O [26]
(f) Channel conductivity	Significantly lower [26]
(g) Channel radius	Dependent on the propagation length [26]

Macroscopic evolutions of repetitively pulsed streamer discharge in humid air from present experiments		
(a) Streamer inception	(1) inception cloud	Smaller, nonlinearly scales with the critical electric field
	(2) shell formation	Much smaller without apparent shell formation
	(3) filamentary break-up	More filamentary channels under 1st voltage pulse
(b) Propagation of primary streamer	(1) 1st voltage pulse	Average velocity decreases with increasing RH
	(2) 2nd voltage pulse	Significantly follow previous secondary streamer trails
(c) Propagation of secondary streamer	(1) channel diameter	Roughly identical in dry air and humid air
	(2) morphology	More illuminating branches from the same root
(e) Thermal effect	Post-discharge heated channels are more pronounced in humid air than dry air	
(g) Withstanding capability	(1) high PRF (>300 Hz)	No significant differences between humid air and dry air
	(2) medium PRF (180–300 Hz)	The decreasing edge shifts towards the high PRF end
	(3) low PRF (<180 Hz)	Saturates at high humidity

exposure capability. It may be validated by the stroboscopic imaging technique or the combination of an intensifier and a high-speed camera.

Present simulations of streamer discharge in humid air are still preliminary. Effects of actual gas temperature changes during the 'pulse-off' period on evolutions of charged species have not been incorporated due to the lack of vibration-translational relaxation mechanisms [10] and experimental temperature curves. Besides, streamer inception and propagation behaviors under following voltage pulses have not been simulated with initial conditions [47]. Furthermore, three-stage evolutions from inception cloud to filamentary break-up may only be revealed in sophisticated 3D models.

4.2. Evolution mechanisms and discharge instabilities in humid under repetitive pulses

Evolution mechanisms of pulse-periodic streamers in humid air are dependent on memory effect and instability mechanisms. Effects of the air humidity on repetitively pulsed streamer discharges are summarized in table 2, including the microscopic influential mechanisms from literature (mainly for the single pulsed streamer discharge) and macroscopic evolution tendencies from current experiments. The main purposes of table 2 are to document observed evolution tendencies and to establish theoretical foundations for evolution mechanisms under repetitive pulses in humid air.

Conventionally, streamer inception dynamics from the needle tip could be divided into three categories, i.e. the inception cloud around the needle tip, shell formation with semi-spherical illuminating fronts, and break-up into filamentary channels. These behaviors before the primary streamer propagations are significantly affected by residual charges. Furthermore, the streamer-to-spark transition is preceded by the prolonging of the secondary streamer towards the grounded electrode (see figures 4 and 6). The effects of the air humidity on evolutions of streamer discharge at high PRF are explained as follows.

(a) *On the streamer inception behaviors*. The streamer filamentation processes are much faster in humid air than in dry air, including the smaller inception cloud and the earlier break-up into filamentary channels. These differences are already apparent under the very first voltage pulse. Chen *et al* and Nijdam *et al* observed that the inception cloud was larger with increasing the O_2 concentration in N_2–O_2 mixtures [19, 20]. Although both the electronegativity of the oxygen molecule and water vapor are bigger than N_2, increasing the water vapor content would not similarly increase the inception cloud. This difference is probably caused by the smooth production of seed electrons through the enhanced photo-ionization process by increasing the O_2 concentration. Nevertheless, the critical breakdown field is higher with increasing the water vapor concentration [44], which would nonlinearly induce the decreasing trend of the maximum radius of the shell phase. The nonlinear dependence may be related to additional instabilities or stochastics induced by water molecules, which is different from the photo-ionization-induced stable formation of the inception cloud [43]. This assumption is also supported by the fact that the number of filamentary streamer channels after the break-up in humid air is approximately twice bigger than dry air (figures 4 and 6).

(b) *On the primary streamer propagation*. The propagation length within the same ICCD exposure slot is longer by approximately 54% in humid air (figure 6(b)-(3)) than in dry air (figure 4(c)-(3)) before breakdown under repetitive pulses. The faster propagation velocity of the primary streamer is not consistent with the traditional assumption that the water vapor with higher electronegativity would impede the streamer propagation. This difference is possibly caused by the variation of the gas density from the enhanced thermal effect in humid air and the longer preservation of hydrated ions from previous discharges.

(c) *On the secondary streamer until the spark breakdown*. The numbers of applied pulses before breakdown at high PRF are approximately identical in humid air and in dry air, which suggests that breakdown behaviors under high-frequency pulses are probably not sensitive to the air humidity. This nonintuitive phenomenon is induced by contrary contributions from (1) hydrated ions with higher electron bound energies (impeding effect) and from (2) the enhanced thermal release to cause higher E/N (facilitating effect). The above contrary influential mechanisms may lead to similar streamer propagation behaviors after several voltage pulses compared with dry air at high PRF, although the secondary streamer in humid air has more illuminating branches originating from the same root.

Nevertheless, quantitative analyses are urgently required in future studies to reveal contributions from residual charged species (from spatial electric field diagnostics) and surplus heat (from the quantitative Schlieren technique).

5. Conclusions

Principal contributions from investigating evolutions of streamer dynamics and discharge instabilities under repetitive pulses in humid air are summarized as follows:

(a) Distinct evolution features of repetitively pulsed streamer discharge in humid air mainly include inception properties and propagation preferences. The filamentary break-up process is earlier and the number of primary streamer channels is significantly bigger in humid air, probably due to more stochastics of the positive streamer filamentation. The primary streamers are more prone to follow the secondary streamer channels under the previous voltage pulse in humid air at higher PRF.

(b) Several similarities of repetitively pulsed streamer discharge in dry and humid air are still present. The conventional shell stage before the filamentation appears under the first pulse in dry air, nevertheless, totally disappears under following pulses at high PRF both in dry and humid air. The streamer-to-spark transition is proceeded by the progressive axial prolongation of secondary streamers with bright heads and faint tails. Unexpectedly, the withstanding capability does not illustrate dramatic differences in dry and humid air at high PRF. More radial expansion and channel branching occur in humid air before the breakdown, although the diameter of the secondary streamer is roughly identical in dry and humid air.

(c) The memory effect mechanisms in humid air are rather complicated than those in dry air. High-density hydrated ions with high electron bound energies residing in the gas gap (possibly impeding streamer propagation instead) and the enhanced thermal release to cause higher E/N (facilitating streamer propagation) contrarily affect evolutions and instabilities of positive streamer discharge in the humid air. The relative contributions from these mechanisms are equally important and both are more persistent than those in dry air. Consequently, evolutions of streamer dynamics and withstanding capability under repetitive pulses in dry and humid air do not illustrate dramatic differences.

A further understanding of evolutions and instabilities of pulse-periodical streamer discharge in humid air could be obtained. Therefore, residual charges transport and energy relaxation are theoretically proposed as two fundamental discharge instability mechanisms and discharge modulation opportunities for repetitive pulses.

Data availability statement

All data that support the findings of this study are included within the article (and any supplementary files).

Acknowledgments

This work was supported by the National Natural Science Foundation of China(52107164, 52077168), the Fundamental Research Funds for the Central Universities (xzy012021015), the China Postdoctoral Science Foundation (2021M702568), and Young Talent Fund of Xi'an Association for Science and Technology. The authors are thankful to Dr Baohong Guo for fruitful discussions concerning simulation validations.

Appendix

A 2D axisymmetric fluid model for the streamer inception and propagation phases was established in a verified fluid framework *Afivo-streamer* [52, 53]. Chemical reactions were obtained from [26, 54, 55] (see the supplementary file) and transport coefficients were computed using *BOLSIG+* [56] with Phelps' cross section for (N_2, O_2) [57] and Morgan's cross section for H_2O [58]. The initial electron and positive ions densities were 10^5 cm^{-3}. The gas temperature and pressure was at 300 K and 0.1 MPa, respectively. The mole fraction of H_2O was 0%, 0.7% (RH = 30%), and 1.4% (RH = 60%). Meanwhile, the simulation for higher temperature (400 K) and higher initial electron density (10^8 cm^{-3}) was also compared. The computational domain and detailed needle/gap dimensions are illustrated in figure A1(a). The applied pulsed voltage

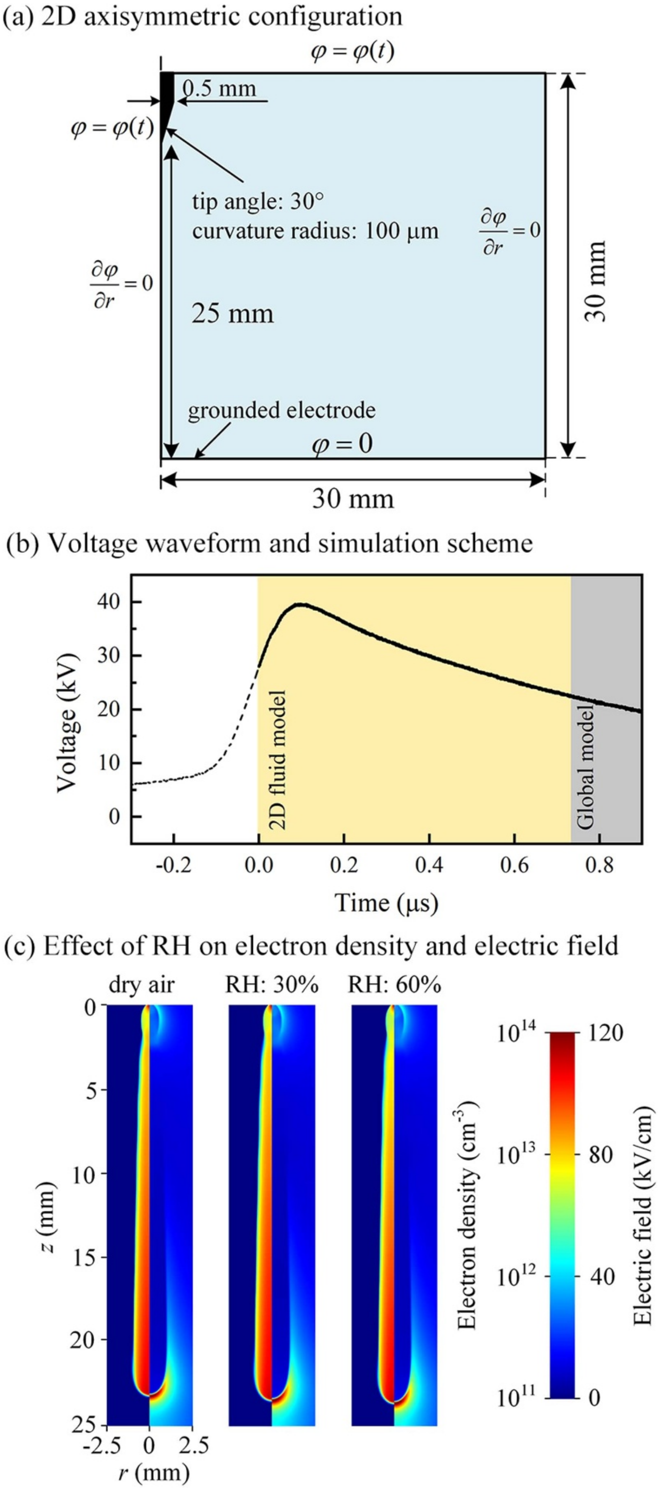

Figure A1. 2D–0D combined simulation configurations and results. (a) 2D axisymmetric simulation configuration. (b) Voltage waveform and simulation scheme. (c) Electron density and electric field distribution in dry and humid air.

is the same as that in the experiment (figure A1(b)). The fluid model simulation starts from the moment when the primary streamer inception was detected in the experiment and reaches the end intentionally when the secondary streamer became stabilized.

A 0D global model simulation with *ZDPlasKin* code [59] and an incorporated BOLSIG+ [56] package was then initiated to obtain evolutions of residual charges during the after-glow stage between two pulses. Initial densities of all species were subtracted from a representative point at the central axis ($r = 0, z = 15$ mm) in the 2D fluid model. The chemical kinetics scheme for humid air was listed in the supplementary file (1041 reactions and 89 species). The gas temperature and pressure were the same as that in the 2D fluid model. The simulation time of the 0D model was 500 μs (i.e. 2 kHz).

Figure A1(c) illustrates spatial distributions of electron density and electric field at the moment before the primary streamer head reaches the plane cathode (t = 34 ns). No significant differences in the electron density and electric field distribution are observed with increasing RH. The same trend is also applicable to the electric field distribution along the primary streamer channel and its propagation velocity (not shown here). Evolutions of streamer dynamics are different in terms of electron density and electric field distribution in dry air and humid air. The electron density in the streamer channel decays much faster with increasing RH because of the enhanced three-body attachment of the O_2 molecule with the presence of H_2O. This tendency is supported by experimental observations in figures 4 and 6. In humid air, the second spike of the emission light intensity from the gap middle is relatively steeper than that in dry air and preceded by a clear dip. Nevertheless, the electron density at the streamer head is not affected by the air humidity probably due to the intensive ionization process as illustrated in simulation results.

ORCID iDs

Zheng Zhao https://orcid.org/0000-0002-7727-7097
Xinlei Zheng https://orcid.org/0000-0002-5993-7450
Anbang Sun https://orcid.org/0000-0003-1918-3110

References

[1] Li H-P, Ostrikov K and Sun W 2018 The energy tree: non-equilibrium energy transfer in collision-dominated plasmas *Phys. Rep.* **770–772** 1–45
[2] Bogaerts A *et al* 2020 The 2020 plasma catalysis roadmap *J. Phys. D: Appl. Phys.* **53** 443001
[3] Jinno R, Komuro A, Yanai H and Ono R 2022 Antitumor abscopal effects in mice induced by normal tissue irradiation using pulsed streamer discharge plasma *J. Phys. D: Appl. Phys.* **55** 17lt01
[4] Ju Y and Sun W 2015 Plasma assisted combustion: dynamics and chemistry *Prog. Energy Combust. Sci.* **48** 21–83
[5] Hasegawa A 1975 *Plasma Instabilities and Nonlinear Effects* (Springer)
[6] Desangles V, Raimbault J-L, Poye A, Chabert P and Plihon N 2019 Pattern formation in low-pressure radio-frequency plasmas due to a transport instability *Phys. Rev. Lett.* **123** 265001
[7] Shao T, Sun G, Yan P and Zhang S 2007 Experimental study of similarity laws in gas breakdown with repetitive nanosecond pulses *Jpn. J. Appl. Phys.* **46** 803–5
[8] Shcherbanev S A, Ding C, Starikovskaia S M and Popov N A 2019 Filamentary nanosecond surface dielectric barrier

discharge. Plasma properties in the filaments *Plasma Sources Sci. Technol.* **28** 065013
[9] Ding C, Khomenko A Y, Shcherbanev S A and Starikovskaia S M 2019 Filamentary nanosecond surface dielectric barrier discharge. Experimental comparison of the streamer-to-filament transition for positive and negative polarities *Plasma Sources Sci. Technol.* **28** 085005
[10] Komuro A and Ono R 2014 Two-dimensional simulation of fast gas heating in an atmospheric pressure streamer discharge and humidity effects *J. Phys. D: Appl. Phys.* **47** 155202
[11] Heitz S A, Moeck J P, Schuller T, Veynante D and Lacoste D A 2016 Influence of air flow parameters on nanosecond repetitively pulsed discharges in a pin-annular electrode configuration *J. Phys. D: Appl. Phys.* **49** 155205
[12] Liu L and Becerra M 2017 Gas heating dynamics during leader inception in long air gaps at atmospheric pressure *J. Phys. D: Appl. Phys.* **50** 345202
[13] Malagón-Romero A and Luque A 2022 Streamer propagation in humid air *Plasma Sources Sci. Technol.* **31** 105010
[14] Norberg S A, Johnsen E and Kushner M J 2015 Formation of reactive oxygen and nitrogen species by repetitive negatively pulsed helium atmospheric pressure plasma jets propagating into humid air *Plasma Sources Sci. Technol.* **24** 035026
[15] Brisset A, Harris B, Dickenson A, Niemi K, Walsh J and Wagenaars E 2022 Effects of humidity on the dynamics and electron recombination of a pin-to-pin discharge in He+H_2O at atmospheric pressure *Plasma Sources Sci. Technol.* **31** 045008
[16] Luo Y, Lietz A M, Yatom S, Kushner M J and Bruggeman P J 2019 Plasma kinetics in a nanosecond pulsed filamentary discharge sustained in Ar-H_2O and H_2O *J. Phys. D: Appl. Phys.* **52** 044003
[17] Aleksandrov N L, Bazelyan E, Ponomarev A and Starikovskiy A 2022 Kinetics of charged species in non-equilibrium plasma in water vapor-and hydrocarbon-containing gaseous mixtures *J. Phys. D: Appl. Phys.* **55** 383002
[18] Zhao Z, Li C, Guo Y, Zheng X, Sun A and Li J 2023 Streamer dynamics and periodical discharge regime transitions under repetitive nanosecond pulses with airflow *Plasma Sources Sci. Technol.* **32** 015002
[19] Nijdam S, Takahashi E, Markosyan A H and Ebert U 2014 Investigation of positive streamers by double-pulse experiments, effects of repetition rate and gas mixture *Plasma Sources Sci. Technol.* **23** 025008
[20] Chen S, Heijmans L C J, Zeng R, Nijdam S and Ebert U 2015 Nanosecond repetitively pulsed discharges in N_2-O_2mixtures: inception cloud and streamer emergence *J. Phys. D: Appl. Phys.* **48** 175201
[21] Zhao Z and Li J 2020 Repetitively pulsed gas discharges: memory effect and discharge mode transition *High Volt.* **5** 569–82
[22] Adamovich I *et al* 2022 The 2022 Plasma Roadmap: low temperature plasma science and technology *J. Phys. D: Appl. Phys.* **55** 373001
[23] Xu P, Zhang B, Chen S and He J 2016 Influence of humidity on the characteristics of positive corona discharge in air *Phys. Plasmas* **23** 063511
[24] Allen N L and Boutlendj M 1991 Study of the electric fields required for streamer propagation in humid air *IEE Proc.* A **138** 37
[25] Mikropoulos P, Stassinopoulos C and Sarigiannidou B 2008 Positive streamer propagation and breakdown in air: the influence of humidity *IEEE Trans. Dielectr. Electr. Insul.* **15** 416–25
[26] Starikovskiy A Y, Bazelyan E M and Aleksandrov N L 2022 The influence of humidity on positive streamer propagation in long air gap *Plasma Sources Sci. Technol.* **31** 114009
[27] Chen X, He W, Du X, Yuan X, Lan L, Wen X and Wan B 2018 Electron swarm parameters and Townsend coefficients of atmospheric corona discharge plasmas by considering humidity *Phys. Plasmas* **25** 063525
[28] Brisset A, Tardiveau P, Gazeli K, Bournonville B, Jeanney P, Ouaras K, Magne L and Pasquiers S 2021 Experimental study of the effect of water vapor on dynamics of a high electric field non-equilibrium diffuse discharge in air *J. Phys. D: Appl. Phys.* **54** 215204
[29] Lietz A M and Kushner M J 2016 Air plasma treatment of liquid covered tissue: long timescale chemistry *J. Phys. D: Appl. Phys.* **49** 425204
[30] Popov N A 2010 Evolution of the negative ion composition in the afterglow of a streamer discharge in air *Plasma Phys. Rep.* **36** 812–8
[31] Ono R, Teramoto Y and Oda T 2010 Effect of humidity on gas temperature in the afterglow of pulsed positive corona discharge *Plasma Sources Sci. Technol.* **19** 015009
[32] Ono R and Oda T 2004 Visualization of streamer channels and shock waves generated by positive pulsed corona discharge using laser Schlieren method *Jpn. J. Appl. Phys.* **43** 321–7
[33] Nakagawa Y, Ono R and Oda T 2011 Density and temperature measurement of OH radicals in atmospheric-pressure pulsed corona discharge in humid air *J. Appl. Phys.* **110** 073304
[34] Sainct F P, Urabe K, Pannier E, Lacoste D A and Laux C O 2020 Electron number density measurements in nanosecond repetitively pulsed discharges in water vapor at atmospheric pressure *Plasma Sources Sci. Technol.* **29** 025017
[35] Aleksandrov N L and Bazelyan E M 1999 Ionization processes in spark discharge plasmas *Plasma Sources Sci. Technol.* **8** 285–94
[36] Aleksandrov N L, Kindysheva S V, Nudnova M M and Starikovskiy A Y 2010 Mechanism of ultra-fast heating in a non-equilibrium weakly ionized air discharge plasma in high electric fields *J. Phys. D: Appl. Phys.* **43** 255201
[37] Lu X and Ostrikov K 2018 Guided ionization waves: the physics of repeatability *Appl. Phys. Rev.* **5** 031102
[38] Li Y, van Veldhuizen E M, Zhang G J, Ebert U and Nijdam S 2018 Positive double-pulse streamers: how pulse-to-pulse delay influences initiation and propagation of subsequent discharges *Plasma Sources Sci. Technol.* **27** 125003
[39] Zhao Z, Huang D D, Wang Y N, He J X, Li C J, Wang Y F and Li J T 2019 Evolution of streamer dynamics and discharge mode transition in high-pressure nitrogen under long-term repetitive nanosecond pulses with different timescales *Plasma Sources Sci. Technol.* **28** 085015
[40] Zhao Z, Huang Z, Zheng X, Li C, Sun A and Li J 2022 Evolutions of repetitively pulsed positive streamer discharge in electronegative gas mixtures at high pressure *Plasma Sources Sci. Technol.* **31** 075006
[41] Ono R and Komuro A 2020 Generation of the single-filament pulsed positive streamer discharge in atmospheric-pressure air and its comparison with two-dimensional simulation *J. Phys. D: Appl. Phys.* **53** 035202
[42] Nijdam S, Wormeester G, van Veldhuizen E M and Ebert U 2011 Probing background ionization: positive streamers with varying pulse repetition rate and with a radioactive admixture *J. Phys. D: Appl. Phys.* **44** 455201
[43] Nijdam S, Teunissen J and Ebert U 2020 The physics of streamer discharge phenomena *Plasma Sources Sci. Technol.* **29** 103001
[44] Kuffel E 1961 Influence of humidity on the breakdown voltage of sphere-gaps and uniform-field gaps *Proc. IEE* A **108** 295

[45] Nemschokmichal S *et al* 2018 Impact of volume and surface processes on the pre-ionization of dielectric barrier discharges: advanced diagnostics and fluid modeling *Eur. Phys. J.* D **72** 89
[46] Höft H, Kettlitz M, Becker M M, Hoder T, Loffhagen D, Brandenburg R and Weltmann K-D 2014 Breakdown characteristics in pulsed-driven dielectric barrier discharges: influence of the pre-breakdown phase due to volume memory effects *J. Phys. D: Appl. Phys.* **47** 465206
[47] Chen X, Zhu Y and Wu Y 2020 Modeling of streamer-to-spark transitions in the first pulse and the post discharge stage *Plasma Sources Sci. Technol.* **29** 095006
[48] Minesi N, Stepanyan S, Mariotto P, Stancu G D and Laux C O 2020 Fully ionized nanosecond discharges in air: the thermal spark *Plasma Sources Sci. Technol.* **29** 085003
[49] Komuro A, Yoshino A, Wei Z and Ono R 2023 Effects of oxygen concentration on streamer propagation and ozone production in a single-filament streamer discharge at atmospheric pressure *J. Phys. D: Appl. Phys.* **56** 185201
[50] Fehsenfeld F C and Ferguson E E 1974 Laboratory studies of negative ion reactions with atmospheric trace constituents *J. Chem. Phys.* **61** 3181
[51] Li X, Dijcks S, Nijdam S, Sun A, Ebert U and Teunissen J 2021 Comparing simulations and experiments of positive streamers in air: steps toward model validation[J] *Plasma Sources Sci. Technol.* **30** 095002
[52] Teunissen J and Ebert U 2017 Simulating streamer discharges in 3D with the parallel adaptive Afivo framework *J. Phys. D: Appl. Phys.* **50** 474001
[53] Teunissen J and Ebert U 2018 Afivo: a framework for quadtree/octree AMR with shared-memory parallelization and geometric multigrid methods *Comput. Phys. Commun.* **233** 156–66
[54] Komuro A, Ono R and Oda T 2013 Behaviour of OH radicals in an atmospheric-pressure streamer discharge studied by two-dimensional numerical simulation *J. Phys. D: Appl. Phys.* **46** 175206
[55] Guo B and Teunissen J 2023 A computational study on the energy efficiency of species production by single-pulse streamers in air *Plasma Sources Sci. Technol.* **32** 025001
[56] Hagelaar G J M and Pitchford L C 2005 Solving the Boltzmann equation to obtain electron transport coefficients and rate coefficients for fluid models *Plasma Sources Sci. Technol.* **14** 722–33
[57] Phelps Database Plasma data exchange project (available at: www.lxcat.net) (Accessed 10 April 2023)
[58] Morgan Database Plasma data exchange project (available at: www.lxcat.net) (Accessed 10 April 2023)
[59] Pancheshnyi S, Eismann B and Hagelaar G 2008 *Computer Code Zdplaskin* (University of Toulouse)